



OPEN

Hydrogen peroxide modification affects the structure and physicochemical properties of dietary fibers from white turnip (*Brassica Rapa* L.)

Qi Gao^{1,3,4}, Xue-jie Zhou^{1,4}, Rui Ma¹, Han Lin¹, Jia-le Wu¹, Xue Peng¹, Masaru Tanokura^{2✉} & You-lin Xue^{1✉}

Turnip (*Brassica rapa* L.) is widely consumed as a vegetable and traditional Chinese medicine with high dietary fiber content. Soluble dietary fiber (SDF) and insoluble dietary fiber (IDF) were obtained from white turnips, and the IDF was modified with alkaline hydrogen peroxide to obtain modified IDF (MIDF) and modified SDF (MSDF). The compositional, structural, and functional properties of the four samples were investigated. After modification, the modified dietary fibers (MDFs) showed smaller particle sizes and lower contents of pectin and polyphenol than those of unmodified dietary fibers (DFs). The results of scanning electron microscopy (SEM), Fourier transformed infrared (FT-IR) spectroscopy, X-ray diffraction (XRD) and differential scanning calorimetry (DSC) showed that compared to the DFs, the MDFs were smaller and had more exposed hydroxyl groups. Analysis of the microrheological behaviors showed that the MDFs had higher viscosity than that of the DFs, with a looser structure for the MSDF and a stable structure for the MIDF. Therefore, due to structural changes, the physical and functional properties of the MDFs were improved compared to those of the unmodified DFs. Pearson correlation analysis showed that the particle size was positively correlated with the pectin content. The water holding capacity (WHC), oil adsorption capacity (OAC) and water swelling capacity (WSC) showed positive correlations with each other. This work indicated that white turnip could be a potential new source of DFs, which presented desirable functional properties after modification.

The cultivation of turnip (*Brassica Rapa* L.) has a long history. As one kind of Cruciferae, turnip is adapted to the adverse environments of the Qinghai-Tibetan Plateau and possesses feeding, edible, and pharmaceutical value, which is highly appreciated as vegetable and traditional Chinese medicine^{1,2}. In addition, it is consumed in enormous quantities not only in Tibet, China, but also throughout the world due to its rich phytochemicals, including glucosinolates, isothiocyanates, polysaccharides, triterpenoids, polyphenols and flavonoids^{3,4}. Pharmacological investigation on turnip revealed the antitumor, antihypertensive, antidiabetic, antioxidant, antiinflammatory, hepatoprotective, and nephroprotective effects⁴. Glucosinolates and isothiocyanates are the main constituents for the protective effect against cancers, while, flavonoids and phenolics are corresponding to the antioxidant effects^{4,5}.

According to the USDA (United States Department of Agriculture) National Nutrient Database (2015), fresh turnip contains 3.5% dietary fiber (DF)⁶. Traditionally, DF has been defined as the varieties of polysaccharide and lignin in the diet that are indigestible by endogenous secretions in the digestive tract⁷. DF is a mixture of cellulose, hemicellulose, gums, lignin and pectin, and can be divided into soluble dietary fiber (SDF) and insoluble

¹College of Light Industry, Liaoning University, No. 66 Chongshan Middle Road, Huanggu District, Liaoning Province, Shenyang 110036, People's Republic of China. ²Department of Applied Biological Chemistry, Graduate School of Agricultural and Life Sciences, The University of Tokyo, 1-1-1 Yayoi, Bunkyo-ku, Tokyo 113-8657, Japan. ³Party School of Liaoning Provincial Party Committee, Shenyang 110161, People's Republic of China. ⁴These authors contributed equally: Qi Gao and Xue-jie Zhou. ✉email: amtanok@mail.ecc.u-tokyo.ac.jp; xueyoulin@lnu.edu.cn

	SDF	MSDF	IDF	MIDF
Yield (%)	20.06 ± 1.77b	11.49 ± 2.50d	51.35 ± 1.89a	19.03 ± 1.99c
Pectin (g/100 g)	6.65 ± 0.50a	1.62 ± 0.35c	6.10 ± 0.65b	0.90 ± 0.42d
Polyphenol (g/100 g)	2.35 ± 0.33a	2.11 ± 0.12b	2.35 ± 0.30a	0.43 ± 0.21c
Protein (g/100 g)	1.70 ± 0.34a	1.72 ± 0.40a	1.05 ± 0.45b	0.97 ± 0.26c
L*	79.22d	98.92a	81.6c	90.27b
a*	8.42a	-0.02d	5.16b	3.47c
b*	20.85a	7.85d	19.02c	19.3b
ΔE	-	1.74b	-	5.29a
WHC (g/g)	-	-	12.75 ± 0.01a	13.65 ± 0.01a
OAC (g/g)	3.29 ± 0.01b	3.71 ± 0.01a	2.29 ± 0.01d	2.41 ± 0.02c
WSC (mL/g)	-	-	5.67 ± 0.06a	5.97 ± 0.05a
Crystallinity (%)	34.19 ± 0.37a	14.84 ± 0.42c	6.76 ± 0.35d	18.71 ± 0.56b
Particle size (d, nm)	488.8 ± 25.73c	397.1 ± 47.99d	3961 ± 101.8a	2810 ± 68.59b
CAB (mg/g)	9.91 ± 0.36b	10.15 ± 0.75a	9.78 ± 0.53c	9.82 ± 0.61bc

Table 1. The yield, basic content, color, WHC, OAC, WSC, crystallinity, particle size, and CAB of DFs from white turnip. Values are the means ± SD of triplicate determinations. The values with a–e indicate significant differences in the same rows, $P < 0.05$. “–” represents not detected.

dietary fiber (IDF)⁸. DF has certain physical characteristics and physiological and bioactive properties, such as capacity to form gels, fermentability, antioxidant activity, viscosity, and the ability to reduce the risk of colon cancer, hypertension, coronary heart disease, diabetes, asthma and obesity, which can be readily applied to food systems as a thickener, emulsifier, stabilizer, and fat replacer^{9,10}.

Usually, DF can be modified by chemical, physical and biological approaches. Chemical modifications (e.g. acid hydrolysis, oxidation, etherification, esterification and cross-linking) may change the DF component as well as the physicochemical properties with extensive washing of material and generating pollutant residues¹¹. Physical methods (e.g. high-pressure homogenization, blasting extrusion, ultrafine grinding, and micro-fluidization) improve the physico-chemical and functional properties of DF by decreasing particle size rather than by increasing SDF content¹². Biological methods are expensive because they require purified enzymes (e.g. cellulose, hemicellulase, xylanase, amylase, amyloglucosidase, alcalase, pepsin, papain, and trypsin) or bacterial strains¹³.

This study focused on the extraction of DFs from white turnips and promoting their functional properties by chemical modification using alkaline hydrogen peroxide, which could react with hemicellulose and lignin to form water-soluble molecules with lower molecular masses than those of the original molecules¹⁴. The structural differences between DFs and modified DFs (MDFs) from white turnip were determined by particle size analysis, scanning electron microscopy (SEM), Fourier transform infrared (FT-IR) spectroscopy, X-ray diffraction (XRD), differential scanning calorimetry (DSC) and microrheological behavior analysis. Furthermore, the capacities of water holding, water swelling, oil adsorption, cation exchange and cholesterol absorption of the samples were also determined to explore the effects of the modification and the potential commercial value and health benefits.

Results and discussion

Basic components, color and granularity analysis. Alkaline hydrogen peroxide could modify the structure of hemicellulose to increase the water solubility, resulting in many differences between the MDFs and DFs¹⁵. The basic components of the DFs are shown in Table 1. The modification treatment resulted in a significant reduction in the pectin content, and the MIDF had the lowest pectin content. For polyphenol, the content decreased after modification, and that in MIDF was the lowest. The protein content of the DF samples was low, and the lowest values were detected in IDF and MIDF. Based on the color measurements, MDFs were obviously whiter than DFs, and MSDF was the whitest, followed by MIDE, IDF and SDF, which was caused by the bleaching effect of hydrogen peroxide¹⁶. The results of particle size analysis showed that modification reduced the particle size.

Structure analyses. *SEM.* As shown in Fig. 1, characteristic honeycomb structure was observed in IDF, and more cracks and holes were detected in MIDE. The SDF particles were large with a rough surface, and a sheet structure was observed. The MSDF particles were relatively smaller with a smoother surface. The microstructure of MDFs was structurally relaxed, and surface wrinkles and cavities were observed. These changes indicated that the modification changed the structure, with some valleys and cracks formed, and the MSDFs were smoother than the SDFs, which resulted in an increase in the number of fiber particles¹⁷. At the same time, many heteropolysaccharides attached to the surface of the particles were detached, which increased the contact area between the hydroxyl groups and the environment¹⁸.

FT-IR. The functional groups and bonding information of the samples could be explained by the FT-IR spectra¹⁷. The FT-IR results are shown in Fig. 2a; the broad peak appearing at 3400 to 3200 cm^{-1} is an O–H stretching vibration derived from hydrogen-bonded alcohol or phenol¹⁸. The MSDF and MIDF showed char-

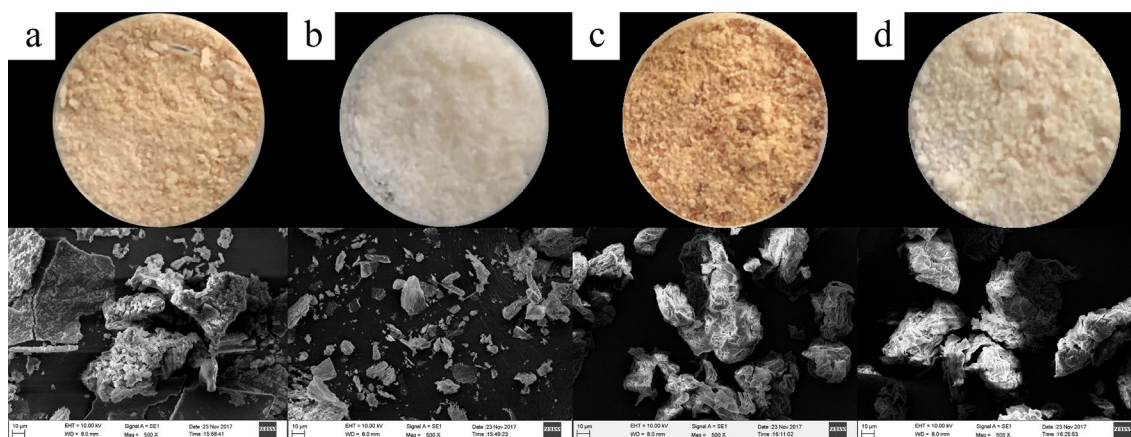


Figure 1. The powder and SEM images (500 \times) of (a) SDF, (b) MSDF, (c) IDF and (d) MIDF obtained from white turnip.

acteristic peaks of free hydroxyl stretching vibrations at 3700–3500 cm^{-1} , indicating that the content of free hydroxyl groups was increased after alkaline hydrogen peroxide modification¹⁸.

A typical $-\text{CH}_2$ stretching vibration was observed at approximately 2920 cm^{-1} , and a $\delta\text{C}-\text{H}$ vibration of $-\text{CH}_2$ was observed at $1465 \pm 20 \text{ cm}^{-1}$. In the fingerprint region, the SDF had a relatively weak peak at 775 cm^{-1} , but this peak shifted to 833 cm^{-1} in MSDF, which indicated that the long chain of $-\text{CH}_2$ groups was broken after the modification and that the content of oligosaccharides was increased¹⁹. SDF and IDF presented a characteristic absorption peak of the benzene ring at 1590–1620 cm^{-1} , and the corresponding peaks were weakened in the MSDF and MIDF samples, which indicated that the original DFs contain more lignin, pectin and hemicellulose²⁰.

A $\text{C}=\text{O}$ stretching vibration was observed in SDF at 1774 cm^{-1} . The corresponding peak of the MSDF was weakened, probably because the $\text{C}=\text{O}$ groups, which are originally present in the fiber, were oxidized²¹.

XRD. Crystalline cellulose exhibits a sharp XRD peak, showing an extended crystal line and complete crystal surface²². As shown in Fig. 2b, broad peaks at 12.5–28 $^\circ$ were observed for IDF and MIDF, and the peak position and width were not significantly different between IDF and MIDF, which indicated the ordered structure of the crystalline region on the cellulose²³. As shown in Table 1, the crystallinity of MSDF (14.84%) was lower than that of SDF (34.19%), and the crystallinity of MIDF (18.71%) was higher than that of IDF (6.76%). According to a previous report, DFs consist of crystalline regions and amorphous regions, and the amorphous regions are composed of noncrystalline cellulose, hemicellulose, and lignin²⁴. The amorphous regions of cellulose is easily destroyed, thus leading to increased relative ratio of crystalline cellulose after hydrolysis²³. As a result, combined with the SEM results, the FT-IR results suggested that the modification damaged the amorphous regions of IDF (Fig. 1), thus leading to the conversion of the amorphous regions into water-soluble components²⁵.

DSC. The exothermic peaks exhibited in the DSC curve illustrate the vaporization of volatile products and the thermal and oxidative decomposition of polymers²⁶. Figure 2c shows the thermal properties of the DFs. In the first temperature range, 50–100 $^\circ\text{C}$, an endothermic peak transition was observed with a maximal peak at approximately 75 $^\circ\text{C}$, which may correspond to the evaporation of unbound water and the phase transition of pectin with sorbed water from crystalline to amorphous structure²⁷. The 2nd endothermic transition of the DFs occurred at approximately 150 $^\circ\text{C}$, which could be explained by the evaporation of bound water in the original DFs²⁸. However, the intensity of the heat flow of DFs was significantly higher than that of MDFs, illustrating that DFs possessed a higher content of bound water. The exothermal peak at 230 $^\circ\text{C}$ might correspond to the pyrolysis peak of pectin²⁹. The heat flow obtained from MDFs was lower than those from DFs, which was consistent with the pectin content (Table 1). The exothermal peaks at approximately 300 $^\circ\text{C}$ were probably the pyrolysis peaks of cellulose, hemicellulose or lignin³⁰. For the MSDF, there is almost no peak after 300 $^\circ\text{C}$, which corresponds to the decreased crystallinity of the MSDF (XRD results). In addition, a higher heat flux strength indicates lower thermal stability, which suggests that MDFs have higher thermal stabilities than DFs³¹.

Physical properties. *Water holding capacity (WHC), water swelling capacity (WSC) and oil adsorption capacity (OAC).* As shown in Table 1, the WHC and WSC of the MIDF increased slightly through modification, which exposed hydroxyl groups in the IDF structure¹³. Second, the hydrolysis of some heteropolysaccharides led to the exposure of more hydroxyl groups, allowing the accommodation of more water molecules. After the modification, the OAC increased, and the OAC of the SDFs was significantly higher than that of the IDFs³². The improvement of these properties indicated a good application prospect of MDFs in food processing.

Cation exchange capability. The curves in Fig. 3a show that practically complete exchange of hydrogen ions occurs in 6 mL of 0.1 M NaOH. For the MSDF, the inflexion point was at 0.5–1.5 mL of NaOH. For the SDF, the inflexion point was in 2–3.5 mL of NaOH. This change indicates that the MSDF has a higher cation exchange

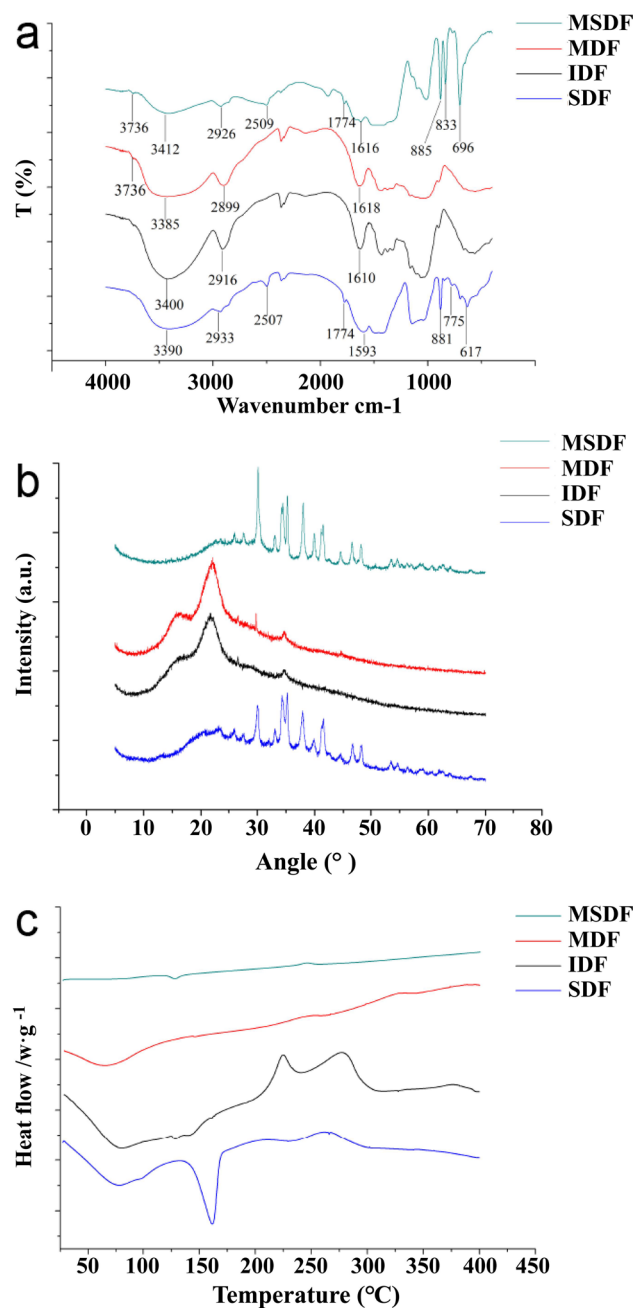


Figure 2. FTIR spectra (a), XRD measurements (b) and DSC analysis (c) of DFs from white turnip.

capacity than that of the SDF. The curves in Fig. 3b show that a practically complete reaction of hydrogen ions occurs in 7 mL of 0.1 M NaOH. This change indicates that the IDF and MIDF showed delayed inflexion points. In conclusion, SDF and MSDF have strong cation exchange capacity, which can effectively control the drastic change in pH³³.

Microrheological properties. Compared with measuring shear rheology, the Rheolaser Lab technique does not modify the DF samples. The Brownian motion of droplets was monitored and interpreted in terms of microrheology³⁴. The motion of the samples was measured, and the interactions of the particles were traced by microrheology, which were expressed as mean square displacements (MSDs) (Fig. 4). The MSD curves of the SDF (Fig. 4a) and IDF (Fig. 4c) were similar. The MSD curve of the MSDF (Fig. 4b) was not linear, indicating that MSDF had viscoelastic properties and that the droplets were free to move due to weak network interactions of droplets³⁵. As shown in Fig. 4d, the MSD curves of the MIDF was linear, indicating that the network interactions of droplets was apparently structurally stable³⁵. Therefore, Fig. 4a,b shows that the configuration of the MSDF apparently was structurally relaxed, and Fig. 4c,d shows that the configuration of the MIDF was structurally stabilized. Alkaline hydrogen peroxide reacted with the IDF, which caused the loss of soluble fractions. Com-

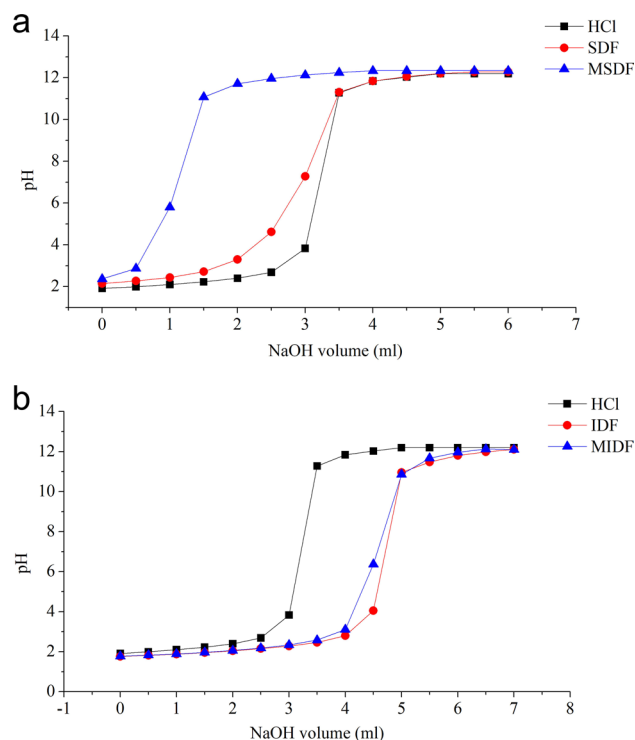


Figure 3. Cation exchange capability of (a) SDFs and (b) IDFs from white turnip.

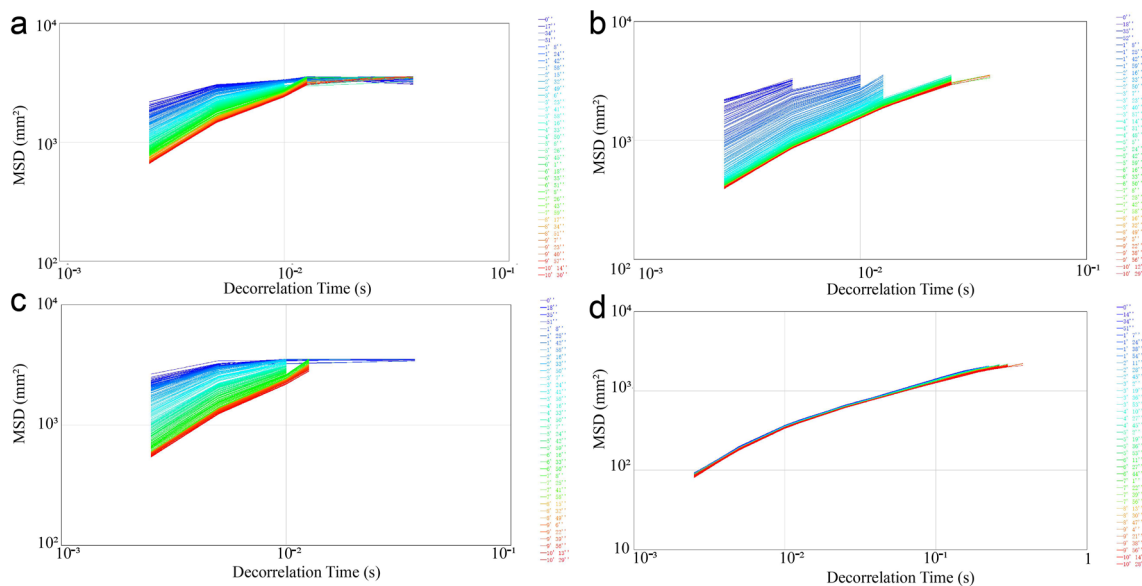


Figure 4. MSD of SDF (a), MSDF (b), IDF (c) and MIDF (d) from white turnip.

bined with the SEM and FT-IR results, the MSDF had smaller particle sizes and more free hydroxyl groups with relatively unstable structures compared to those of the other samples.

As shown in Fig. 5, the macroscopic viscosities of the DFs were represented by the macroscopic viscosity index (MVI) values, which corresponds to the inverse of the speed of the particles for long times³⁵. The viscosity of the MIDF was the highest, followed by that of the MSDF, SDF, and IDF.

Due to the modification, the viscosity of MDFs increased. The peroxide-initiated free radicals reacted with the hydroxyl groups of the fiber and the matrix, and good fiber matrix adhesion along the interface occurred²¹. First, intermolecular hydrogen bond cleavage led to more exposure of polar groups in the molecule, and the charge on the surface of the molecule increased, thereby enhancing the electrostatic interaction among the molecules, as well as between the molecule and the solvent, and increasing the flow resistance of the solution. The increase in

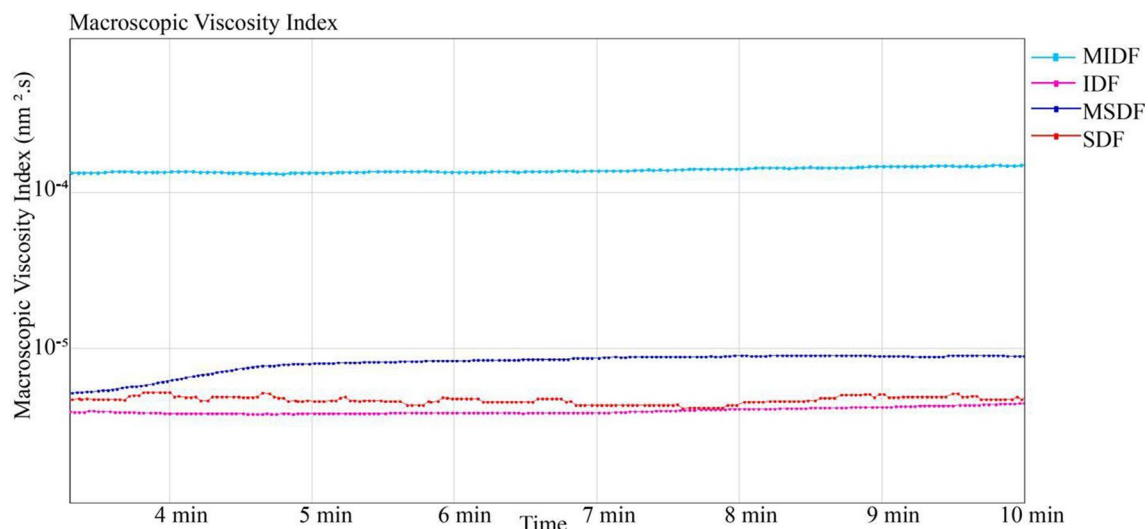


Figure 5. Macroscopic viscosity index of DFs from white turnip. The figure was generated by RheoSoft Master 1.4.0.0.

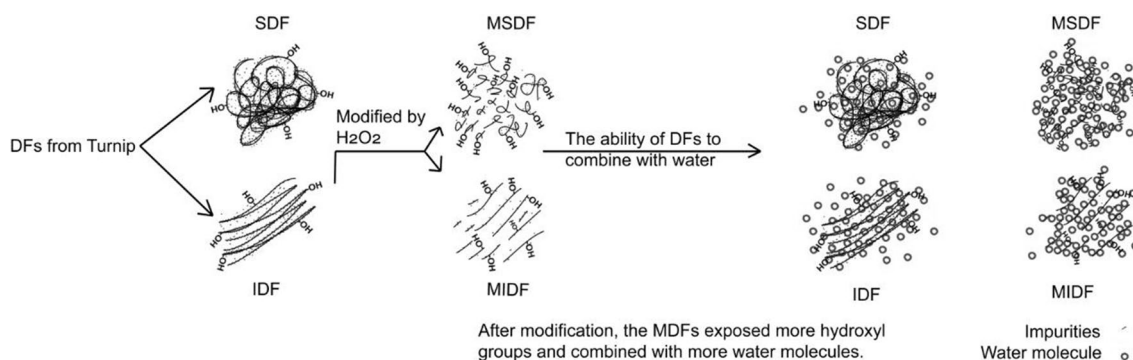


Figure 6. Possible mechanism for the better ability of MDFs to combine with water. The figure was generated by RheoSoft Master 1.4.0.0.

molecular surface charge also thickened the solvation layer of the molecule, which led to further dilation of the molecule and an increase in the viscosity of the solution²⁹. Second, the modification treatment reduced the size of the fiber particles and smoothed them, which increased the effective area of the fiber surface and resulted in more particle interactions and an enhanced network structure with water molecules, resulting in a significant increase in apparent viscosity³⁶. The difference between the MIDF and MSDF was that the crystallinity of the MIDF was higher and that its surface contained more valleys, fiber bundles and gullies (Fig. 1), which increased the effective area of the fiber surface and led to a higher viscosity of the MIDF than of the MSDF³⁷. For the SDF and IDF, the former had a smaller particle size and higher crystallinity, which means a higher effective area of the fiber surface and greater number of fiber bundles, resulting in the viscosity of the SDF being higher than that of the IDF (Fig. 6).

Cholesterol absorption ability (CAB). As shown in Table 1, the MSDF (10.15 ± 0.75) had the strongest CAB, the SDF (9.91 ± 0.36) performed better than the MIDF (9.82 ± 0.61), and the IDF (9.78 ± 0.53) showed the lowest CAB. From the SEM images (Fig. 1), many valleys were cracked or broken after the modification, which resulted in the better CAB of the MDFs. The FT-IR results indicated that the SDF had more hydroxyl groups, indicating that more cholesterol was combined and absorbed.

Correlation analysis among the various properties of DFs. Pearson coefficients were calculated for the various properties of the DFs (Table 2). The pectin and polyphenol contents negatively correlated with the WHC, and the WSC and particle size positively correlated with the pectin content. The modification could destroy the cross-linked structures of polysaccharides from the cell wall and remove pectin, polyphenol and other components, which brought about an increased relative content of cellulose and smaller particle size. The SEM analysis indicated that the modification caused the breakage of the amorphous regions; thus, the crystallinities of the MDFs increased³⁰. Therefore, the higher effective area of the fiber surface and the higher content of cellulose led to a higher WHC and WSC¹⁴. The WHC, OAC and WSC showed a positive correlation with each other, and the particle size showed a negative correlation with the WHC, OAC, and WSC, which indicated that

	Yield	Pectin	Polyphenol	Protein	L*	a*	b*	ΔE	WHC	OAC	WSC	Crystallinity
Pectin	0.591*											
Polyphenol	0.310	0.732*										
Protein	-0.576*	0.190	0.581*									
L*	-0.601*	-0.873*	-0.310	0.151								
a*	0.354	0.812**	0.248	0.020	-0.96**							
b*	0.457	0.538	-0.178	-0.439	-0.880**	0.873**						
ΔE	1.000**	-0.985**	-0.999**	-0.999**	-1.000**	1.000**	1.000**					
WHC	-0.999**	-1.000**	-0.999**	-0.741	1.000**	-1.000**	1.000**	0				
OAC	-0.716**	-0.102	0.427	0.949**	0.447	-0.277	-0.667*	-1.000*	1.000**			
WSC	-0.999**	-1.000**	-0.999**	-0.741	1.000**	1.000**	1.000**	0	1.000**	1.000**		
Crystallinity	-0.554	0.244	0.02	0.578*	-0.329	0.579*	0.342	1.000**	1.000**	0.43	1.000**	
Particle size	0.609*	0.759**	0.116	-0.320	-0.979**	0.934**	0.954**	1.000**	-0.998**	-0.593*	-0.998**	0.284

Table 2. Pearson correlation coefficients among different properties of DFs from turnip. * $P \leq 0.05$; ** $P \leq 0.01$.

a smaller particle size led to a higher WHC, WSC and OAC. The FT-IR results indicated that intramolecular hydrogen bonding interactions were broken and that the content of oligosaccharides was increased³⁰. The MDFs showed weaker water evaporation peaks in the DSC curves and exhibited better microrheological properties than those of the DFs, with the properties correlated with the WSC and WHC. These results revealed that compared to unmodified DFs, the MDFs exhibited modified structures, crystallinity regions, and functional groups with better performance in terms of functional properties¹³. Therefore, these MDFs have potential applications in food and health products as functional ingredients.

Conclusion

In conclusion, this study revealed changes in the compositional, structural, and functional properties of DFs. The SEM, FT-IR, XRD and DSC results showed that compared to the unmodified DFs, the MDFs had decreased particle sizes and more exposed functional groups that influenced their functional properties, such as •OH groups. The microrheological properties of the DFs showed that the MSDF network was structurally relaxed and that the MIDF network was structurally stable, which was verified by the structure analyses. Overall, our research suggests that turnip could be a good source of DFs and that MDFs have wider application prospects in food systems.

Materials and methods

Materials. White turnips were obtained from the Daliangshan region of Sichuan Province. The turnips were washed under running water and then sliced and immersed in 1.5% sodium chloride and 0.2% citric acid solution for 20 min. Next, the slices were put into a dry oven (GZX-9076MBE, Shanghai Boxun Industry & Commerce Co., Ltd., Shanghai, China) and dried at 60 °C. The dried slices were powdered by a pulverizer (SZ-500A-3, Yongkang Shanzhu Trading Co., Ltd., Zhejiang, China) and then sieved through an 80 mm sieve.

Reagents. Mesophilic amylase (enzyme activity $\geq 100,000$ U/g solid powder) was obtained from Jiangsu Ruiyang Biotechnology Co., Ltd., Suzhou, China. All reagents used in this work were of analytical reagent grade unless otherwise stated.

Extraction of DFs. Turnip powders (20 g) were mixed with distilled water (1:4), and the pH was adjusted to 5.4 by using 5 mol/L NaOH. Then, mesophilic amylase (0.3%) was added to remove starch in a 65 °C water bath with stirring for 1 h. Next, the exact solution was mixed with 100 ml of 7% NaOH in a 65 °C water bath with continuous stirring for 45 min to remove protein. The mixture was centrifuged at 6000 rpm for 20 min (TG16G Changsha Yingtai Instrument Co., Ltd., Changsha, China). The obtained precipitate was first washed with distilled water and 95% ethanol, dried at 40 °C in a drying oven and then pulverized to obtain the IDF powder. For the supernatant, 4 volumes of 95% ethanol were added with gentle stirring, and then, the mixture was left overnight to precipitate SDF. The precipitate, which was obtained after filtering, was redissolved in distilled water (1:1) and then was lyophilized (SCIENTZ-10N Xinzhi Biotechnology Co., Ltd., Ningbo, China). The obtained powder was weighed to calculate the yield of SDF. The yields were calculated as follows:

$$\text{The yield of SDF (\%)} = \frac{\text{the weight of dried SDF (g)}}{\text{the weight of dried turnip powder (g)}} \times 100\%$$

$$\text{The yield of IDF (\%)} = \frac{\text{the weight of dried IDF (g)}}{\text{the weight of dried turnip powder (g)}} \times 100\%$$

Modification of IDF (Fig. 6). IDF was modified to obtain the MIDF and MSDF³⁸. IDF was soaked in 10% H₂O₂ (pH 11.5) with a solid–liquid ratio of 1:20 (g/mL) under ultrasound sonication at 200 W and 40 °C for 2 h (TH-400 BQ, Jining Tianhua Ultrasonic Electronic Instrument Co., Ltd., Shandong, China). Then, the mixture was centrifuged at 6000 rpm for 20 min. The obtained precipitate was then washed with distilled water and 95%

ethanol and dried at 60 °C to obtain the MIDE. The supernatant was precipitated with 4 volumes of 95% ethanol and left overnight. The precipitate was then lyophilized to obtain the MSDF. The yields were calculated as follows:

$$\text{The yield of MSDF(\%)} = \frac{\text{the weight of dried MSDF(g)}}{\text{the weight of dried turnip powder(g)}} \times 100\%$$

$$\text{The yield of MIDE(\%)} = \frac{\text{the weight of dried MIDE(g)}}{\text{the weight of dried turnip powder(g)}} \times 100\%$$

Basic composition and granularity analysis. The moisture (method 925.09), protein (method 955.04) and ash (method 942.05) contents were measured by AOAC official methods³⁹. The pectin content was measured by the carbazole colorimetric method. The polyphenol content was determined by the Folin–Ciocalteu method.

The average particle sizes of the DF samples were measured by a laser particle size analyzer (Nano ZS90, Malvern Instruments Ltd., England).

Structure analyses. *SEM.* The microstructure of DFs was observed by a Zeiss EVO10 field emission scanning electron microscope (JSM-5610LV, JEOL, Japan). The dehydrated samples were placed on a metal stage and coated with a 10 nm gold layer.

FT-IR. DF was mixed with spectroscopic grade potassium bromide (KBr) powder and then pelletized to 1 mm. Four different DF samples were measured by a Fourier transform infrared spectrophotometer (FT/IR3000, Jasco, Japan) to obtain the FT-IR spectra from 400 to 4000 cm⁻¹.

XRD. X-ray diffractometry was performed on a Bruker D8 Advance X-ray diffractometer (Bruker, AXS, Germany) with Cu radiation at 40 kV and an incident current of 30 mA. The angular region ranging from 5° to 70° was scanned with a step length of 0.02° and a step rate of 0.2 s/step. The degree of crystallinity was calculated using the MDI Jade 5.0 software (Materials Data, Inc., California, USA)¹³.

DSC. The thermal properties of DFs were analyzed using a differential scanning calorimeter (DSC1, Mettler Toledo, USA). A sample (5–10 mg) was placed into an aluminum pan and immediately covered with a aluminum cover. The calorimeter was calibrated using indium with an empty aluminum pan used as a reference. The sample pans were heated from 25 °C to 400 °C at a rate of 10 °C/min³⁰.

Physical properties. *Color measurement.* The color characteristics (L*, a* and b*) of DFs were determined using a colorimeter (NR20XE, 3nh Co., China), and the results were expressed in terms of the CIELAB system.

WHC. The WHC of DF was measured by the method of Sowbhagya et al. (2007)⁴⁰. DF (IDE and MIDE) powder (0.04 g) was hydrated in 3 mL of distilled water at 25 °C for 2 h and then centrifuged at 3000 rpm for 20 min. Then, the fresh weight of the residue was recorded. The WHC was calculated by the following equation:

$$\text{WHC(g/g)} = (m_f - m)/m$$

where m_f is the weight of the fresh residue (g) and m is the dry weight of the sample powder (g).

WSC. The WSC was calculated by the method of Sowbhagya et al. (2007) with some modifications⁴⁰. DF (IDE and MIDE) powder (0.2 g) was hydrated in 10 mL of distilled water in a graduated test tube at 25 °C for 24 h. The volume of DFs was recorded, and the WSC was calculated by the following equation:

$$\text{WSC(mL/g)} = (v_1 - v_0)/w_0$$

where v_1 is the volume of the hydrated DF, v_0 is the volume of the DF before hydration, and w_0 is the weight of the DF before hydration.

OAC. The OAC was calculated by the method of Abdul-Hamid and Luan (2000) with some modifications⁴¹. DF (IDE, SDF, MIDE and MSDF) powder (0.12 g) was mixed with 3 mL of soya bean oil for 1 h at 37 °C. The mixture was centrifuged at 3000 rpm for 20 min. The OAC was determined based on the amount of soya bean oil retained by the DF:

$$\text{OAC(g/g)} = (m_r - m) \times 100/m$$

where m_r is the residue weight, which contained the oil (g), and m is the original weight of the DF (g).

Cation exchange capability. The cation exchange capability was calculated by the method of Chau and Huang (2003) with slight modifications³³. DF (IDE, SDF, MIDE and MSDF) powder (0.3 g) was dissolved in 30 mL of 0.01 mol/L HCl and was refrigerated at 4 °C overnight, which was set as the control group. After the temperature reached 25 °C, 0.5 mL of 0.1 mol/L NaOH was added to the mixture to achieve complete cation exchange, and the pH change of the solution was recorded.

Microrheological behavior. A commercial Rheolaser Master (Formulation, l'Union, France), which was based on diffusing-wave spectroscopy (DWS), was used for measuring the microrheology of the DFs. This technique is similar to dynamic light scattering and measures the Brownian motion of particles, which depends on the viscoelastic structure of the sample. Aqueous solutions of 40% (w/v) SDF and MSDF and 5% (w/v) suspensions of IDF and MIDF were measured at 25 °C. The instrument measures Brownian motion of the particle as the droplet mean square displacement (MSD) versus time. MVI parameters of the samples were obtained with the software RheoSoft Master 1.4.0.0³⁵.

CAB. The cholesterol absorption abilities of the samples were determined according to a previous study³. First, a 0.5 g sample (IDF or MIDF) or 0.1 g sample (SDF or MSDF) was dissolved in 25 mL of 1 mg/mL cholesterol solution. The reaction mixture was incubated in a water bath at 37 °C for 2 h, followed by centrifugation (4000 × g for 20 min). Then, the cholesterol content of 0.1 mL of supernatant was tested by the phthalic aldehyde method at 550 nm.

Statistical analyses. Each experiment was carried out in triplicate, and the data are expressed as the mean ± standard deviation (SD). Pearson correlation coefficients (r) were calculated for the various physicochemical properties, and the least significant difference (LSD) test was compared by SPSS 10.0 software; $P < 0.05$ was considered statistically significant.

Received: 2 May 2020; Accepted: 15 December 2020

Published online: 13 January 2021

References

- Liang, Y. S. *et al.* Identification of phenylpropanoids in methyl jasmonate treated *Brassica rapa* leaves using two-dimensional nuclear magnetic resonance spectroscopy. *J. Chromatogr. A* **1112**, 148–155 (2006).
- Fernandes, F. *et al.* Chemical and antioxidative assessment of dietary turnip (*Brassica rapavar. rapa* L.). *Food Chem.* **105**, 1003–1010 (2007).
- Xie, Y. *et al.* Composition analysis and anti-hypoxia activity of polysaccharide from *Brassica rapa* L. *Int. J. Biol. Macromol.* **47**, 528–533 (2010).
- Paul, S., Geng, C.-A., Yang, T.-H., Yang, Y.-P. & Chen, J.-J. Phytochemical and health-beneficial progress of turnip (*Brassica rapa*): health beneficial progress of turnip. *J. Food Sci.* **84**, 19–30 (2019).
- Arora, R., Arora, S. & Vig, A. P. Development of validated hightemperature reverse-phase UHPLC-PDA analytical method for simultaneous analysis of natural isothiocyanates in cruciferous vegetables. *Food Chem.* **239**, 1805–1089 (2018).
- USDA National Nutrient Database for Standard Reference Release 1 April, 2018 Full Report (All Nutrients) February 25, 23:11 EST. <https://fdc.nal.usda.gov/fdc-app.html#/food-details/170466/nutrients> (2019).
- Trowell, H. *et al.* Dietary fibre redefined. *The Lancet* **307**, 967 (1976).
- Arora, S. K., Patel, A. A., Kumar, N. & Chauhan, O. P. Determination of relationship between sensory viscosity rating and instrumental flow behavior of soluble dietary fibers. *J. Food Sci. Technol.* **53**, 2067–2076 (2016).
- Chen, J. *et al.* Physicochemical and functional properties of dietary fiber from maca (*Lepidium meyenii* Walp.) liquor residue. *Carbohydr. Polym.* **132**, 509–512 (2015).
- Sozer, N., Cicerelli, L., Heiniö, R. L. & Poutanen, K. Effect of wheat bran addition on in vitro starch digestibility, physico-mechanical and sensory properties of biscuits. *J. Cereal Sci.* **60**, 105–113 (2014).
- Park, K. H., Lee, K. Y. & Lee, H. G. Chemical composition and physicochemical properties of barley dietary fiber by chemical modification. *Int. J. Biol. Macromol.* **60**, 360–365 (2013).
- Ma, M. M. & Mu, T. H. Modification of deoiled cumin dietary fiber with laccase and cellulase under high hydrostatic pressure. *Carbohydr. Polym.* **136**, 87–94 (2016).
- Ma, M. M. & Mu, T. H. Effects of extraction methods and particle size distribution on the structural, physicochemical, and functional properties of dietary fiber from deoiled cumin. *Food Chem.* **194**, 237–246 (2016).
- Maes, C. & Delcour, J. A. Alkaline hydrogen peroxide extraction of wheat bran non-starch polysaccharides. *J. Cereal Sci.* **34**, 29–35 (2001).
- Sangnark, A. & Noomhorm, A. Chemical, physical and baking properties of dietary fiber prepared from rice straw. *Food Res. Int.* **37**, 66–74 (2004).
- Abegunde, O. K., Mu, T. H., Chen, J. W. & Deng, F. M. Physicochemical characterization of sweet potato starches popularly used in Chinese starch industry. *Food Hydrocolloids* **33**, 169–177 (2013).
- Li, N., Feng, Z., Niu, Y. & Yu, L. Structural, rheological and functional properties of modified soluble dietary fiber from tomato peels. *Food Hydrocolloids* **77**, 557–565 (2018).
- Liu, L., Chen, H. & Pan, D. Modification of polyacrylonitrile precursor fiber with hydrogen peroxide. *Fibers Polymers* **13**, 587–592 (2012).
- Hussein, A. O., Mohammed, G. J., Hadi, M. Y. & Hameed, I. H. Phytochemical screening of methanolic dried galls extract of *Quercus infectoria* using gas chromatography-mass spectrometry (GC-MS) and Fourier transform-infrared (FT-IR). *J. Pharmacogn. Phytotherapy* **8**, 49–59 (2016).
- Fung, W. Y., Yuen, K. H. & Liang, M. T. Agrowaste-based nanofibers as a probiotic encapsulant: fabrication and characterization. *J. Agric. Food Chem.* **59**, 8140–8147 (2011).
- Kabir, M. M., Wang, H., Lau, K. T. & Cardona, F. Chemical treatments on plant-based natural fibre reinforced polymer composites: an overview. *Compos. B Eng.* **43**, 2883–2892 (2012).
- Cleven, R., van den Berg, C. & van der Plas, L. Crystal structure of hydrated potato starch. *Starch-Stärke* **30**, 223–228 (1978).
- Nyman, E. M. G. L. & Svanberg, S. M. Modification of physicochemical properties of dietary fibre in carrots by mono- and divalent cations. *Food Chem.* **76**, 273–280 (2002).
- Zhao, X. *et al.* Surface characterization of corn stalk superfine powder studied by FTIR and XRD. *Colloids Surf., B* **104**, 207–212 (2013).
- Alfred, D., Cintron, M. S. & Santiago, M. Cellulose polymorphism, crystallite size, and the segal crystallinity index. *Cellulose* **20**, 583–588 (2013).
- Mudgil, D., Barak, S. & Khatkar, B. S. X-ray diffraction, IR spectroscopy and thermal characterization of partially hydrolyzed guar gum. *Int. J. Biol. Macromol.* **50**, 1035–1039 (2012).
- Slavov, A., Panchev, I., Kovacheva, D. & Vasileva, I. Physico-chemical characterization of water-soluble pectic extracts from *rosa damascena*, *calendula officinalis*, and *matricaria chamomilla* wastes. *Food Hydrocolloids* **61**, 469–476 (2016).

28. Zhang, W. *et al.* Properties of soluble dietary fiber-polysaccharide from papaya peel obtained through alkaline or ultrasound-assisted alkaline extraction. *Carbohydr. Polym.* **172**, 102–112 (2017).
29. Wang, L., Yuan, F., Xiang, J. & Gao, Y. Functional properties and rheology of soluble dietary fiber from citrus slag. *Chin. J. Food Sci.* **3**, 24–31 (2015) ((in Chinese)).
30. Wen, Y., Niu, M., Zhang, B., Zhao, S. & Xiong, S. Structural characteristics and functional properties of rice bran dietary fiber modified by enzymatic and enzyme-micronization treatments. *LWT-Food Sci. Technol.* **75**, 344–351 (2017).
31. Osorio, C., Carriazo, J. G. & Barbosa, H. Thermal and structural study of guava (*Psidium guajava* L.) powders obtained by two dehydration methods. *Química Nova* **34**, 636–640 (2011).
32. Yang, C., Wang, Y. & Chen, L. Fabrication, characterization and controlled release properties of oat protein gels with percolating structure induced by cold gelation. *Food Hydrocolloids* **62**, 21–34 (2017).
33. Chau, C. F. & Huang, Y. L. Comparison of the chemical composition and physicochemical properties of different fibers prepared from the peel of *Citrus sinensis* L. Cv. Liucheng. *J. Agric. Food Chem.* **51**, 2615–2618 (2003).
34. Corredig, M. & Alexander, M. Food emulsions studied by DWS: recent advances. *Trends Food Sci. Technol.* **19**, 67–75 (2008).
35. Xu, D., Aihemaiti, Z., Cao, Y., Teng, C. & Li, X. Physicochemical stability, microrheological properties and microstructure of lutein emulsions stabilized by multilayer membranes consisting of whey protein isolate, flaxseed gum and chitosan. *Food Chem.* **202**, 156–164 (2016).
36. Cardoso, M. A. P. *et al.* Oat fibers modification by reactive extrusion with alkaline hydrogen peroxide. *Polímeros* **26**, 320–326 (2016).
37. Sébastien, R. *et al.* Development of gelling properties of inulin by microfluidization. *Food Hydrocolloids* **24**, 318–324 (2010).
38. Wang, H. O. *et al.* Treatment with hydrogen peroxide improves the physicochemical properties of dietary fibres from Chinese yam peel. *Int. J. Food Sci. Technol.* <https://doi.org/10.1111/ijfs.14405> (2019).
39. AOAC. *Official Methods of Analysis* (Association of Official Analytical Chemists, Washington, DC, 2000).
40. Sowbhagya, H. B., Suma, P. F., Mahadevamma, S. & Tharanathan, R. N. Spent residue from cumin—a potential source of dietary fiber. *Food Chem.* **104**, 1220–1225 (2007).
41. Abdul-Hamid, A. & Luan, Y. S. Functional properties of dietary fibre prepared from defatted rice bran. *Food Chem.* **68**, 15–19 (2000).

Acknowledgements

This work was supported by the National Natural Science Foundation of China (31201285), the China Postdoctoral Science Foundation (2017M611752), the Liaoning Revitalization Talents Program (XLYC1807270), the Science and Technology Support Program from Shenyang City (17136800) and the College Student Innovation and Entrepreneurship Development Program of Liaoning University (X201810140247).

Author contributions

Y. X. and M. T. designed and supervised the project. Q. G., X. Z., R. M. and H. L. conducted the experiments, analyzed the results, and drafted the manuscript. J. W., X. P. and Y. X. revised the manuscript.

Competing interests

The authors declare no competing interests.

Additional information

Correspondence and requests for materials should be addressed to M.T. or Y.X.

Reprints and permissions information is available at www.nature.com/reprints.

Publisher's note Springer Nature remains neutral with regard to jurisdictional claims in published maps and institutional affiliations.



Open Access This article is licensed under a Creative Commons Attribution 4.0 International License, which permits use, sharing, adaptation, distribution and reproduction in any medium or format, as long as you give appropriate credit to the original author(s) and the source, provide a link to the Creative Commons licence, and indicate if changes were made. The images or other third party material in this article are included in the article's Creative Commons licence, unless indicated otherwise in a credit line to the material. If material is not included in the article's Creative Commons licence and your intended use is not permitted by statutory regulation or exceeds the permitted use, you will need to obtain permission directly from the copyright holder. To view a copy of this licence, visit <http://creativecommons.org/licenses/by/4.0/>.

© The Author(s) 2021